

Lawrence S. Taylor, PhD
 Deborah J. Rubens, MD
 Brian C. Porter, PhD
 Zhe Wu, PhD
 Raymond B. Baggs, DVM,
 PhD
 P. Anthony di Sant'Agnes,
 MD
 Gyongyi Nadasdy, MD
 David Pasternack, BS
 Edward M. Messing, MD
 Priya Nigwekar, MD
 Kevin J. Parker, PhD

Published online before print
 10.1148/radiol.2373041573
 Radiology 2005; 237:981-985

Abbreviations:

DRE = digital rectal examination
 PSA = prostate-specific antigen
 3D = three-dimensional

¹ From the Departments of Biomedical Engineering (L.S.T.) and Electrical and Computer Engineering (B.C.P., Z.W., K.J.P.), University of Rochester, 240 Hutchison Rd, Rm 205, Rochester, NY 14627-0126; Departments of Radiology (D.J.R.), Laboratory Animal Medicine (R.B.B.), Pathology and Laboratory Medicine (P.A.d.S., P.N.), Environmental Medicine, Strong Memorial Hospital (D.P.), and Urology (E.M.M.), University of Rochester School of Medicine and Dentistry, Rochester, NY; and Department of Pathology, Ohio State Medical Center, Columbus, Ohio (G.N.). Received September 10, 2004; revision requested November 14; revision received December 20; accepted January 21, 2005. Supported in part by NIH grant no. 5 R01 AG016317-03. Address correspondence to K.J.P. (e-mail: rcbu@ece.rochester.edu).

See Materials and Methods for pertinent disclosures.

Author contributions:

Guarantors of integrity of entire study, L.S.T., D.J.R.; study concepts/study design or data acquisition or data analysis/interpretation, all authors; manuscript drafting or manuscript revision for important intellectual content, all authors; approval of final version of submitted manuscript, all authors; literature research, L.S.T., D.J.R.; clinical studies, all authors; statistical analysis, L.S.T., B.C.P., Z.W., R.B.B., D.P., K.J.P.; and manuscript editing, L.S.T., D.J.R., B.C.P., Z.W., R.B.B., P.A.d.S., E.M.M., K.J.P.

© RSNA, 2005

Prostate Cancer: Three-dimensional Sonoelastography for in Vitro Detection¹

PURPOSE: To prospectively evaluate the accuracy of three-dimensional (3D) sonoelastographic imaging, relative to that of gray-scale ultrasonography (US), in the in vitro detection of prostate cancer.

MATERIALS AND METHODS: The study was approved by the institutional review board and was HIPAA compliant. Informed consent was obtained from all patients. Nineteen prostatectomy specimens from patients aged 46–70 years with biopsy-proved prostate cancer were scanned in three dimensions by using conventional B-mode US and sonoelastography with vibrations of more than 100 Hz. Step-sectioned whole-mount histologic specimens were used to create a 3D volume of the prostate and the tumors within it. B-mode US scans and regions of low vibration on the sonoelastographic images (hard regions) were formatted in three dimensions. The lesions in the 19 cases were classified into two groups, as follows: G1 lesions were pathologically confirmed tumors with a volume of at least 1.0 cm³, and G2 lesions were pathologically confirmed tumors smaller than 1.0 cm³. G1 lesions were evaluated with B-mode US and sonoelastography and classified as true-positive, false-positive, true-negative, or false-negative; G2 lesions were evaluated only with sonoelastography. Findings at histologic examination were used as the reference standard. True-positive findings necessitated 3D lesion correlation between pathologic and imaging data. Conventional definitions of accuracy and sensitivity were used for statistical analysis.

RESULTS: For G1 lesions (seven lesions with a volume of at least 1.0 cm³), sonoelastography had an accuracy of 55% and a sensitivity of 71% and B-mode US had an accuracy of 17% and a sensitivity of 29%. The mean tumor volume was 3.1 cm³ ± 2.1 (standard deviation). For G2 lesions (22 lesions with a volume of less than 1.0 cm³), the mean tumor volume was 0.32 cm³ ± 0.21. Sonoelastography had an accuracy of 34% and a sensitivity of 41%; there were six false-positive findings.

CONCLUSION: Sonoelastography performed considerably better than did gray-scale US in the depiction of prostate cancer for tumors with volumes of more than 1 cm³.

© RSNA, 2005

Early and accurate detection of prostate cancer is an urgent priority because it is the most prevalent type of cancer in men and the second most frequent cause of cancer deaths in men. New prostate cancer cases in the United States for 2004 were estimated at 23 110, and deaths were estimated at 29 900 (1).

Current screening of serum prostate-specific antigen (PSA) levels and with digital rectal examination (DRE) followed by ultrasonographically (US)-guided prostate biopsy have some substantial shortcomings. Transrectal US depicts only 64% of cancers per gland (2) and 32%–42% of cancers per lobe (3,4). With random biopsy, up to 32% of cancers are missed when comparing biopsy results per lobe with prostatectomy specimens (3). These invisible cancers are as important as those visible at transrectal US (5). In PSA-screened populations, the per patient accuracy of transrectal US was only 52% owing to the large number of false-positive findings encountered (6). In this same group, DRE, which helps

detect stiffness, was specific (82%) but insensitive (50%) in the detection of prostate cancer. DRE is limited anatomically to the posterior gland and cannot help detect lesions confined anteriorly or in the transition zone, where as many as 28% of cancers occur (7). Given the limitations in transrectal US-guided prostate biopsy, a technique that improves imaging and biopsy yield of prostate cancer would be beneficial.

PSA screening commonly results in biopsy in men with serum PSA levels of more than 4.0 ng/mL and in younger men or those at high risk with PSA levels of more than 2.5 ng/mL (8,9). Biopsy is performed in 8%–15% of men (10,11) aged 50–70 years, and the cancer yield is 22% (10). Those negative for cancer undergo repeat PSA screening and may undergo repeat biopsy at 6–12 months, which yields another 12% with cancer (12). This process incurs both increased costs and delays in diagnosis (10–12). Thus, improvements to transrectal US and biopsy procedures are valuable.

DRE is used for prostate cancer screening because many cancers are hard at palpation. During the past 15–20 years, several research groups have investigated various imaging techniques called elasticity imaging or elastography (13). This method takes advantage of the difference in the stiffness (shear modulus) between healthy and diseased tissue. Because many cancers have an elevated shear modulus, the interest in estimating the elastic (mechanical) properties of tissue and in imaging hard tumors has grown during the past decade. Currently, techniques for elasticity imaging can be separated into five methods: magnetic resonance (MR) elastography (14), sonoelastography or vibration imaging (15), elastography or strain imaging (16), remote palpation (17), and transient elastography (18).

The purpose of our study was to prospectively evaluate the accuracy of three-dimensional (3D) sonoelastographic imaging in the *in vitro* detection of prostate cancer and compare it with that of gray-scale US.

MATERIALS AND METHODS

Support for this study, in the form of a loaned B-scan imaging system (Logiq-7), was received from GE Medical Systems, Milwaukee, Wis. The authors had control of all data and information submitted for publication.

Sonoelastographic images are vibra-

tion amplitude images in which stiff regions (those with a high elastic modulus) appear as areas of low vibration relative to the surrounding softer tissue, which transmits vibration more readily (19). Color Doppler US is used to display the vibration differences, with high vibration displayed as bright green and low vibration as dark green. The Doppler image is overlaid on the gray-scale image, which permits simultaneous coregistered image acquisition. A stiff lesion causes a local decrease in the vibration field, which is displayed as a void or dark region on the color Doppler image.

Gland Selection and Reference Standard

Excised glands were selected from patients with prostate cancer who (a) were scheduled to undergo radical prostatectomy (so that 3D histologic slices could be obtained as the reference standard), (b) had a palpable lesion at DRE or at least one core specimen that was 50% positive for tumor at preoperative biopsy, and (c) did not undergo hormonal or radiation therapy. The patients ranged in age from 46 to 70 years, with an average age of 60.5 years. This study was approved by our institutional review board and was compliant with the Health Insurance Portability and Accountability Act. Informed consent was obtained for the use of the excised gland. Nineteen glands were selected from November 2001 through August 2003.

The selection criteria did not include patients with prostate cancer in whom the tumor volume was estimated to be less than approximately 1 cm³ and others in whom the entire prostate and tumor had been treated with radiation or hormonal therapy, which alters the gland stiffness and the amount of residual tumor. Also eliminated from the study were those rare patients with a tumor so advanced as to leave questionable “normal” regions.

Scanning

The details of the scanning protocol and the blinded reading protocol were as follows: Specimens were obtained immediately after surgical excision, embedded in 3.4% agar gel, and imaged with a 3D protocol. Coregistered sonoelastographic and B-mode US images were obtained at 1-mm spacing by using a linear 7-MHz probe (model 739L; GE Medical Systems) mounted on a motorized track (Velmex, Bloomfield, NY). Images were obtained

by two authors (L.S.T. and Z.W.) with 2 years of experience in sonoelastographic imaging. Vibration was performed from a source opposite the probe, with frequencies of 100–300 Hz. A combination of frequencies (chords) was used to diminish artifacts (19). The highest frequency that adequately penetrated the tissue to give a uniform vibration field was chosen.

Pathologic Evaluation

After US, the fresh prostate gland was weighed and measured to determine the maximum dimension in all three planes from apex to base, transversely, and anteroposteriorly. The resection margins of the gland were inked with different colors that represented each quadrant. A landmark device, which consisted of two sets of four 3-mm-diameter mating metal prongs, was inserted into the specimen through the apex and base to provide fiducial markers. After fixation, the gland was remeasured to assess shrinkage, sliced into 4-mm-thick sections from the apex to the base, and digitally photographed. After being photographed, the tissues from the Petri dishes were transferred to cassettes and embedded in paraffin (Paraplast; Sherwood Medical, St Louis, Mo) to make blocks that were sliced into 4–5- μ m-thick sections and placed on glass slides.

The microscopic whole-mount sections were examined by one of three pathologists (P.A.d.S., G.N., and P.N., all with more than 5 years of experience in pathology). The pathologists were blinded to the results at sonoelastography. Areas of carcinoma and benign nodular hyperplasia were outlined with two different color-marking pens, and the slides were submitted for 3D volume reconstruction. Digital photographs of each gross prostate slice and its accompanying histologic slide were processed with a computer program (Photoshop, version 5.5; Adobe, San Jose, Calif) by aligning each planar image with the puncture holes from the landmark device to generate the 3D reconstructions.

Reference Standard

Transverse 1-mm B-mode US scans were used to create a 3D image of the surface of the prostate. In each two-dimensional section, the boundary of the gland was outlined by B.C.P. and Z.W. to differentiate the gland from the background. The sequence of boundary outlines was reconstructed in three dimensions and used as the reference standard

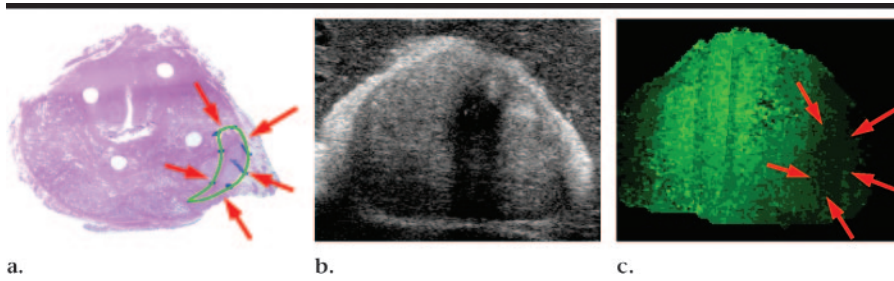


Figure 1. Two-dimensional transverse images of a confirmed case of cancer in the midgland. The rectal surface is posterior. (a) Histologic image shows the cancer (arrows), which was outlined in green by the pathologist. (Hematoxylin-eosin stain.) (b) Gray-scale US scan obtained in the same plane as a. The cancer is not visible. (c) Sonoelastographic image corresponding to b. There is a deficit in vibration (arrows), which is indicative of an area of stiffer tissue.

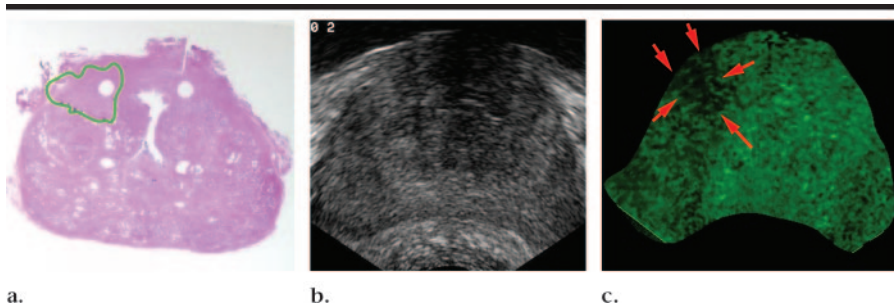


Figure 2. In vivo two-dimensional sonoelastographic image coregistered with a histologic slide. Images are all transverse; the rectal surface is posterior. (a) Histologic slide shows cancer anterior and on the patient's left, outlined in green. (b) Gray-scale B-mode US scan is normal. (c) Sonoelastographic image corresponding to b has a dark vibration deficit (arrows) anteriorly and on the left, which corresponds to the pathologically evident cancer in a. Note that the B-mode US scan does not show cancer in that region.

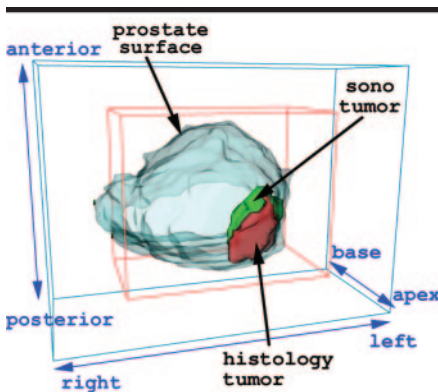


Figure 3. Three-dimensional reconstruction of prostate cancer within the gland surface. The prostate surface (transparent blue) was reconstructed from B-mode US data; tumor data from sonoelastography (*sono*) and histologic evaluation are indicated by arrows.

for the true shape of the gland and the baseline volume because the US scans are unaffected by tissue fixation and cassette preparation.

Registration of the US and pathology volumes was achieved by identifying the

prostate surface and urethra, which is visible at the midgland level of the prostate anterior to the verumontanum. Registration accuracy was assessed by B.C.P. by measuring urethral offset and also by an overlap metric of intersection over union applied to the whole gland (20). Fusion was achieved with an in-house correlative program (21), and images were viewed with IRIS Explorer (Numerical Algorithms Group, Downers Grove, Ill), as described previously (21,22). The best 3D correlation maps the gray-scale B-mode data into the histologic frame of reference. The largest lesion in each gland seen at sonoelastography or gray-scale US was compared with the histologic specimen.

Scoring

US and sonoelastographic images were scored prospectively and independently by two observers (D.J.R., who scored the B-mode US scans, and L.S.T., who scored the sonoelastographic images) while blinded to the findings at initial transrectal US, DRE, or pathologic examination.

Pathology reports and sections were reviewed by three authors (P.A.d.S., G.N., or P.N.), who were blinded to the findings at US or sonoelastography, for tumor presence, size, and location. Locations, volumes, and types of adenomatous nodules (stromal or glandular) were recorded.

Sonoelastographic images were considered positive for tumor when a contiguous localized 3D vibration deficit was present for more than 2 mm in the craniocaudal direction. Sonoelastographic imaging defects could be focal (well circumscribed with no vibration) or diffuse (poorly margined with green pixels [vibration] incompletely filling in the gray-scale image). B-mode US scans were considered positive for tumor when a discrete 3D hypoechoic nodule or region was identified or if there was a local mass of any echogenicity disrupting the gland contour. Three-dimensional coregistered pathologic, B-mode US, and sonoelastographic images were displayed as a 3D volume fusion with pathologic lesions in red, sonoelastic lesions in green, and overlap between pathologic and sonoelastographic lesions in bright yellow. In addition, sequential transverse two-dimensional images were examined. Pathologic and sonoelastographic lesion volumes, locations, and overlap measures were also recorded.

Statistical Analysis

The following definitions were used to record results within the 3D coregistered volumes: A true-positive finding was recorded for a local region of the prostate volume when a discrete lesion of pathologically confirmed cancer had substantial (approximately 50% or more) coregistration with a discrete lesion seen at sonoelastography or B-mode US. A false-positive finding was recorded for a local region of the prostate volume when a discrete lesion seen at sonoelastography or B-mode US had less than 50% coregistration with a pathologically confirmed cancer. A false-negative finding was recorded when a discrete cancer had no corresponding lesion at sonoelastography or B-mode US. A true-negative finding was recorded only if there was no cancer at pathologic examination and no lesion at sonoelastography or B-mode US.

In the data analysis, the total number of identified lesions was defined as the number of true-positive, true-negative, false-positive, and false-negative lesions; accuracy was determined by dividing the number of true-positive and true-negative findings by the total number of lesions; sensitivity was determined by di-

viding the number of true-positive findings by the number of true-positive and false-negative findings; and positive predictive value was calculated by dividing the number of true-positive findings by the number of true- and false-positive findings.

RESULTS

An example of a sonoelastographic void is shown in Figure 1. This approach is also applicable to in vivo clinical examination, as shown in Figure 2. The coregistration of B-mode surface, sonoelastography lesions, and pathology lesions in three dimensions is shown in Figure 3. A breakdown of the 3D coregistration into a sequence of stacked two-dimensional sections (1-mm thickness) is shown in Figure 4.

The results for both lesion groups are shown in Table 1. The average tumor volume (\pm standard deviation) for G1 lesions as determined at histologic examination was $3.0 \text{ cm}^3 \pm 2.1$. The average G1 tumor volume at sonoelastography, with use of only the five true-positive findings, was $2.8 \text{ cm}^3 \pm 1.8$. The average volume of the five histologic lesions to which they corresponded was $3.7 \text{ cm}^3 \pm 2.2$. The mean volume of the sonoelastographic tumors in this group was 93% of the mean histologically confirmed tumor volume. The mean size of the 22 histologically confirmed G2 lesions was $0.32 \text{ cm}^3 \pm 0.21$.

The ratio of intersection to union of whole-gland volumes ranged from 0.69 to 0.82 (20,21). A complete description of the 3D image registration protocol has been published elsewhere (21).

Within the 19 prostates evaluated were 29 discrete foci of cancer. These cancers ranged in volume from a maximum of 6.6 cm^3 to less than 0.1 cm^3 . One prostate was found to have no pathologically confirmed cancer (within the limits of our 3-mm sampling of pathology slices); in addition, no lesions were seen at sonoelastography. This case was the only true-negative finding in the study.

By using sonoelastography, seven G1 lesions (pathologically confirmed focal lesions with a tumor volume of at least 1 cm^3) were scored as five true-positive and two false-positive findings. In two cases, the lesion seen at sonoelastography did not match the pathologic tumor; these lesions were considered false-negative findings. Thus, the sensitivity was 71%, the accuracy was 55%, and the positive predictive value was 71%. Similarly, gray-



Figure 4. Four adjacent transverse cross sections (with a 1-mm gap between sections) from a 3D fusion volume show the overlapping sonoelastographic and histologic tumor regions. The prostate surface as reconstructed with B-mode US data is white; histologic data are in yellow. The red region is the histologically derived tumor, and the green region is the sonoelastographically derived tumor. The overlapping regions within the prostate are in yellow. The rectal surface is posterior.

scale (B-mode) US of the G1 lesions yielded two true-positive, five false-positive, and five false-negative findings; there were no true-negative findings. From this small sample, we find that the accuracy was 17% (two of 12 lesions), sensitivity was 29% (two of seven lesions), and positive predictive value was 29% (two of seven lesions). The results are shown in Table 2.

At sonoelastography of G2 lesions (22 pathologically confirmed tumors with volumes of less than 1 cm^3), there were nine true-positive findings, 13 false-negative findings, six false-positive findings, and one true-negative finding. Thus, the sensitivity was 41%, the accuracy was 34%, and the positive predictive value was 60%.

DISCUSSION

The results of this study demonstrate that, in the examination of a whole gland for cancer, the sensitivity and accuracy with sonoelastography could be increased to levels of 71% and 55%, respectively, which are major improvements over the levels reported with conventional B-mode US. These results, however, are for a relatively small group of whole prostatectomy specimens ($n = 7$) with a focal tumor with a volume of more than 1.0 cm^3 .

The accuracy and sensitivity of sonoelastography were much poorer, however, for cases in which the individual cancers were smaller than 1.0 cm^3 . Results of our previous work have shown that the contrast on sonoelastographic images of lesions diminishes with decreasing frequency (23,24). Many G2 tumors are too small to generate sonoelastographic contrast at the frequencies we are currently using. In addition, as the size of the cancer approaches 0.1 cm^3 , we lack an understanding of the mechanical and elastic properties of the tumor and

TABLE 1
Comparison of Findings at Sonoelastography and Histologic Examination

Finding	Lesion Type	
	G1	G2
No. of true-positive	5	9
No. of false-positive	2	6
No. of true-negative	0	1
No. of false-negative	2	13
Accuracy (%)	55	34
Sensitivity (%)	71	41
Positive predictive value (%)	71	60

TABLE 2
Comparison of Findings at B-Mode US and Histologic Examination of G1 Lesions

Finding	Value
No. of true-positive	2
No. of false-positive	5
No. of true-negative	0
No. of false-negative	5
Accuracy (%)	17
Sensitivity (%)	29
Positive predictive value (%)	29

whether there is sufficient mechanical contrast in comparison with surrounding tissues to make a detectable void on a sonoelastographic image. It is possible that the stiffness of very small tumors may not be the same as that of larger tumors; the stiffness could be considerably less, especially compared with that of background tissue. Additional research into the biomechanical properties of prostate cancer is needed to provide the baseline data about this fundamental issue.

For G1 lesions, B-mode US values for prostate cancer detection are lower than those in other published studies (2-4);

this may be due to our stricter requirement of substantial 3D coregistration to qualify as a true-positive finding. Comparison of in vitro transverse scanning versus real-time biplanar transrectal US introduces another issue in that longer real-time imaging and imaging in more than one plane may improve lesion detection.

Another factor in the poor accuracy and sensitivity in both groups was the prevalence of false-positive findings. Further analysis of the 3D images demonstrates that some of the false-positive voids seen on sonoelastographic images are owing to calcifications or to regions of benign prostate hyperplasia, as confirmed at histologic examination. It is reasonable to hypothesize that calcified regions will manifest as “hard” sonoelastographic voids because these are easily visualized on the B-mode scan; these voids are straightforward to eliminate in practice. Not much is known, however, about the elastic properties of benign prostate hyperplasia—either the stromal or the glandular types. More information about this is needed because the gray-scale US appearance of a benign prostate hyperplasia nodule also overlaps with that of cancer. Additional difficulties may be encountered in translating the results of this in vitro study to in vivo conditions, where patient motion and access constraints are present.

Finally, the comparison of volumes (3D sonoelastographic vs pathologic) is imprecise because of the coarse sampling of the whole specimens into 4-mm pathology specimens, compared with the 1-mm US scan acquisition. In addition, factors including tissue shrinkage and warping during preparation and the need for manual outlining of the pathologic slides contribute to the imprecise volume estimates from pathologic examination.

In conclusion, 3D sonoelastographic imaging of prostate cancer currently shows promise for the in vitro evaluation of lesions larger than 1 cm³ and an improvement over gray-scale US. False-positive

findings occur with calcifications (and can potentially be corrected by referencing the gray-scale US scan) and adenomatous nodules, which currently cannot be differentiated from cancer with gray-scale US or sonoelastography. The number of false-negative findings increases as the tumor size decreases, and this may be due to the underestimation of tumor size with sonoelastography and the limited image contrast resolution at the frequencies applied. Future work will require better understanding of the mechanical properties of tissue, the stiffness differential between tumor and normal tissue needed to provide image contrast, and the development of alternative vibration techniques to generate higher frequency shearwaves at depth.

References

- Jemal A, Tiwari RC, Murray T, et al. Cancer statistics, 2004. *CA Cancer J Clin* 2004; 54(1):8–29.
- Ellis JH, Tempany C, Sarin MS, Gatsonis C, Rifkin MD, McNeil BJ. MR imaging and sonography of early prostatic cancer: pathologic and imaging features that influence identification and diagnosis. *AJR Am J Roentgenol* 1994;162(4):865–872.
- Slonim SM, Cuttino JT Jr, Johnson CJ, et al. Diagnosis of prostatic carcinoma: value of random transrectal sonographically guided biopsies. *AJR Am J Roentgenol* 1993;161:1003–1006.
- Coffield KS, Speights VO, Brawn PN, Riggs MW. Ultrasound detection of prostate cancer in postmortem specimens with histological correlation. *J Urol* 1992;147:822–826.
- Ellis WJ, Brawer MK. The significance of isoechoic prostatic carcinoma. *J Urol* 1994; 152:2304–2307.
- Rubens DJ, Gottlieb RH, Maldonado CE Jr, Frank IN. Clinical evaluation of prostate biopsy parameters: gland volume and elevated prostate-specific antigen level. *Radiology* 1996;199(6):159–163.
- Reissigl A, Pointner J, Strasser H, Ennemoser O, Klocker H, Bartsch G. Frequency and clinical significance of transition zone cancer in prostate cancer screening. *Prostate* 1997;30(2):130–135.
- Smith RA, von Eschenbach AC, Wender R, et al. American Cancer Society guidelines for the early detection of cancer: update of early detection guidelines for prostate, colorectal, and endometrial cancers. *CA Cancer J Clin* 2001;51(1):38–75.
- Barry MJ. Prostate-specific antigen testing for early diagnosis of prostate cancer. *N Engl J Med* 2001;344(18):1373–1377.
- Catalona WJ, Smith DS, Ratliff TL, et al. Measurement of prostate-specific antigen in serum as a screening test for prostate cancer. *N Engl J Med* 1991;324:1156–1161.
- Brawer MK, Chetner MP, Beattie J, Buchner DM, Vessela RL, Lange PH. Screening for prostatic carcinoma with prostate specific antigen. *J Urol* 1992;147:841–845.
- Catalona WJ. Screening for prostate cancer: enthusiasm. *Urology* 1993;42(2):113–115.
- Gao L, Parker K, Lerner RM, Levinson SF. Imaging of the elastic properties of tissue: a review. *Ultrasound Med Biol* 1996;22(8): 959–977.
- Muthupillai R, Lomas DJ, Rossman PJ, Greenleaf JF, Manduca A, Ehman RL. Magnetic resonance elastography by direct visualization of propagating acoustic strain waves. *Science* 1995;269(5232):1854–1857.
- Lerner RM, Huang SR, Parker KJ. “Sonoelasticity” images derived from ultrasound signals in mechanically vibrated targets. *Ultrasound Med Biol* 1990;16(3):231–239.
- Ophir J, Garra B, Kallel F, et al. Elastographic imaging. *Ultrasound Med Biol* 2000;26(suppl 1):S23–S29.
- Nightingale K, Soo MS, Nightingale R, Trahey G. Acoustic radiation force impulse imaging: in vivo demonstration of clinical feasibility. *Ultrasound Med Biol* 2002;28(2):227–235.
- Catheline S, Wu F, Fink M. A solution to diffraction biases in sonoelasticity: the acoustic impulse technique. *J Acoust Soc Am* 1999;105(5):2941–2950.
- Taylor LS, Porter BC, Rubens DJ, Parker KJ. Three-dimensional sonoelastography: principles and practices. *Phys Med Biol* 2000; 45(6):1477–1494.
- Porter BC, Taylor L, Baggs R, et al. Histology and ultrasound fusion of excised prostate tissue using surface registration. *IEEE Ultrason Symp Proc* 2001;2:1473–1476.
- Porter BC, Rubens DJ, Strang JG, Smith J, Totterman S, Parker KJ. Three-dimensional registration and fusion of ultrasound and MRI using major vessels as fiducial markers. *IEEE Trans Med Imaging* 2001;20(4): 354–359.
- Taylor LS, Porter BC, Nadasdy G, et al. Three-dimensional registration of prostate images from histology and ultrasound. *Ultrasound Med Biol* 2004;30(2):161–168.
- Rubens DJ, Hadley MA, Alam SK, Gao L, Mayer RD, Parker KJ. Sonoelasticity imaging of prostate cancer: in vitro results. *Radiology* 1995;195(2):379–383.
- Parker KJ, Fu D, Gracewski SM, Yeung F, Levinson SF. Vibration sonoelastography and the detectability of lesions. *Ultrasound Med Biol* 1998;24(9):1437–1447.